Title
Geospatial uncertainty-aware road classification from remote sensing for hazard management

Journal
Remote Sensing Applications Society and Environment, 42

ISSN
2352-9385

Authors
Solgi, Ryan
Mayes, Marc
Hazard, Rob
et al.

Publication Date
2026-04-01

DOI
10.1016/j.rsase.2026.102068

Peer reviewed

Remote Sensing Applications: Society and Environment 42 (2026) 102068

Contents lists available at ScienceDirect

Remote Sensing Applications: Society and Environment

journal homepage: www.elsevier.com/locate/rsase

Geospatial uncertainty-aware road classification from remote sensing for hazard management

Ryan Solgi [a,b,*], Marc Mayes [c,d], Rob Hazard [e], Hugo A. Loáiciga [a]

[a] Department of Geography, University of California, Santa Barbara, CA, USA
[b] Department of Electrical and Computer Engineering, University of California, Santa Barbara, CA, USA
[c] Spatial Informatics Group – Natural Assets Laboratory (SIG-NAL), Santa Barbara, CA, USA
[d] Earth Research Institute, University of California, Santa Barbara, CA, USA
[e] Santa Barbara County Firesafe Council, Santa Barbara, CA, USA

ARTICLE INFO

Keywords:
Road width
Bayesian classification
Remote sensing
Hazard management

ABSTRACT

Natural hazards such as wildfires and floods are becoming increasingly frequent and severe, increasing the need for effective evacuation and emergency planning. A key aspect of this planning is ensuring that road infrastructure can support emergency response and safe evacuations. In this study, we introduce a novel geospatial uncertainty-aware road detection (GUARD) method to identify road segments of substandard width from remote sensing data. GUARD leverages airborne optical imagery and light detection and ranging (LiDAR) data for road region extraction and applies a Bayesian classification model with moment-based features to account for measurement uncertainty. By identifying substandard road segments for follow-up inspection, GUARD can facilitate more efficient road infrastructure monitoring and emergency planning. Evaluation using ground-truth data from a case study in Santa Barbara, California, United States, demonstrates the method's effectiveness. Results indicate that a significant portion of the road segments in the study area have passages narrower than required standards. This finding highlights the potential vulnerability of many older wildland–urban interface neighborhoods and how the GUARD method can contribute to road infrastructure monitoring and adaptation in emergency planning.

1. Introduction

During natural hazards such as wildfires, hurricanes and floods, roads play a central role in emergency evacuation and response. With climate change progressing, the frequency of extreme weather events is increasing (Intergovernmental Panel on Climate Change (IPCC), 2021). Hazards such as wildfires and floods are becoming more common and severe, posing significant threats to communities. Effective evacuation and emergency planning are paramount in mitigating the impact of these disasters. Previous incidents in the United States of America (USA), such as the 2005 Hurricane Katrina in New Orleans, the 2018 Camp Fire in Paradise, and Lahaina's deadly 2023 wildfire in Hawaii have highlighted the critical importance of developing and maintaining robust evacuation routes in disaster-prone areas (Wolshon, 2006; Maranghides et al., 2023; Sommer, 2024).

Identifying key transportation-related evacuation issues is a part of policies and practices for emergency evacuation in response to natural hazards (Wolshon et al., 2005). Previous work has studied evacuation analyses in response to hazard management using traffic and human behavior modeling (Aldahlawi et al., 2024; Effinger, 2021; Chen et al., 2020). Meanwhile, remote sensing has

* Corresponding author at: Department of Geography, University of California, Santa Barbara, CA, USA.
E-mail address: ryan.solgi@geog.ucsb.edu (R. Solgi).

https://doi.org/10.1016/j.rsase.2026.102068
Received 21 January 2026; Received in revised form 5 May 2026; Accepted 16 May 2026

Available online 23 May 2026

been widely applied for monitoring the state of natural hazards (Szpakowskia et al., 2021; Sadiq et al., 2022; Sdraka et al., 2024; Salandra et al., 2024; Alizadeh et al., 2024; Beyki et al., 2025) and in emergency management (Rahman et al., 2021; Zheng et al., 2021; Vishwanath et al., 2023; Sibandze et al., 2025). Studying resilience and vulnerability of road networks and their connectivity in hazard management is an emerging topic (Wei and Xu, 2024; Niu et al., 2022; Moratalla and Uma, 2023; Dye et al., 2021; Bhattacharyya et al., 2023); however, studies that utilize remote sensing to evaluate roads against required standards in the context of natural hazard management are limited.

Monitoring and extracting road information using remote sensing has been the topic of many previous studies with applications in urban planning, infrastructure management, autonomous driving, and hazard management (Wang et al., 2019; Zhou et al., 2020; Chen et al., 2021; Karimzadeh et al., 2022; Lian et al., 2020; Ouyang et al., 2025; Malama et al., 2024). Machine learning models have advanced road extraction, yet challenges persist in accurately capturing road features from a bird's-eye view due to noise and occlusions (Lian and Huang, 2022). In particular, the extraction of road boundaries, such as curbs and road widths, from remote sensing data has been a persistent problem, complicated by the limited availability of open-access data, which hinders the development of robust methods (Hu et al., 2024).

Sufficient road width is crucial for ensuring the efficient movement of both residents and emergency vehicles. Emergency response organizations have established standards regarding roadway width (e.g., Division (2021)). Adequate width prevents bottlenecks, reduces congestion, and facilitates simultaneous access and egress, enhancing the effectiveness of evacuation efforts and potentially saving lives. Many roads do not meet evacuation standards, categorizing them as substandard. Infrastructure development is often constrained by time, cost, terrain and land acquisition challenges. Given these constraints, continuous monitoring and assessment of evacuation routes are essential for identifying weak spots and taking necessary planning and precautionary actions for emergency management.

Although remote sensing facilitates monitoring and assessment of roads (Schnebele et al., 2015), detecting narrow passages remains challenging due to various sources of error and uncertainty. Numerous methods have been developed for road extraction and width estimation from remote sensing data; however, their performance can be affected by challenges such as occlusions (e.g., vegetation and shadows), segmentation errors, and geometric distortions (Z. Chen et al., 2022). These challenges make it difficult to detect narrow roads reliably from remote sensing images.

In this study, we formulate the problem of substandard road detection as a classification problem. We introduce a novel geospatial uncertainty-aware road detection (GUARD) method designed to classify substandard road segments using airborne optical imagery and light detection and ranging (LiDAR) data. The GUARD method estimates the width of the road and applies a Bayesian model enhanced with moment transformation to predict the likelihood of road classes while accounting for measurement uncertainties. This method serves as a preliminary tool to identify road segments requiring detailed in-situ inspections for pre-disaster assessment, thereby increasing efficiency for emergency planning. Although the individual components of GUARD (e.g., segmentation and width estimation) are modular, the novelty lies in their integration into an uncertainty-aware, segment-level probabilistic framework for hazard-oriented road assessment. Due to the lack of publicly available road width data, we collected in-situ ground-truth data in the Mission Canyon neighborhood of Santa Barbara, California, USA, to evaluate the model and assess road conditions.

2. Related work

2.1. Road segmentation

Previous works have studied a wide range of methods for road extraction and segmentation from remote sensing data (Z. Chen et al., 2022). Traditional approaches including knowledge-based systems, active contour models, and optimization methods have been utilized in extracting roads from remote sensing images (Wang et al., 2016; Yin et al., 2015; Matkan et al., 2014). Machine learning methods such as neural networks (NNs) have been successfully applied to road segmentation tasks (Song and Civco, 2004; Kirthika and Mookambiga, 2011). More recently, deep learning techniques, including convolutional neural networks (CNNs), generative adversarial networks (GANs), and transformers, have gained significant popularity for road segmentation from optical remote sensing images due to their ability to capture complex features and patterns (Zhong et al., 2016; Zhang et al., 2018; Jiang et al., 2022; Abdollahi et al., 2020; W. Chen et al., 2022).

The requirement for massive amounts of training data complicates the application of deep learning methods in road segmentation and extraction. One study addressed this issue by generating synthetic data using GANs (Shamsolmoali et al., 2021). Additionally, semi-supervised, weakly-supervised, and unsupervised methods have been proposed to alleviate this challenge (Liu et al., 2022). In semi-supervised techniques, the model is trained using a limited number of labeled images (Chen et al., 2023). Weakly-supervised road segmentation, on the other hand, involves training the model with limited and imprecisely labeled data, such as image-level tags, scribbles (centerlines), or sparse point annotations, thereby reducing the need for extensive manual labeling (Wu et al., 2019; H. Chen et al., 2022; Hu et al., 2021; Wei and Ji, 2022; Lian and Huang, 2022).

Unsupervised learning addresses the challenge of road segmentation and extraction in target areas without labeled data. A previous study (Miao et al., 2014) developed a semi-automatic method utilizing the geodesic method, kernel density function, and mean shift to extract centerlines using user-provided seed points. Another study introduced an unsupervised-restricted deconvolutional neural network, which involved pretraining with unlabeled data followed by unsupervised feature extraction for road segmentation (Tao et al., 2017). Additionally, one study developed an unsupervised model based on GANs for road map extraction and road segmentation (Song et al., 2021). An unsupervised domain adaption (UDA) model using GAN was developed to address domain shift problem in road segmentation with limited labeled data (Zhan et al., 2021). Another study developed a topology-aware unsupervised method for domain-adaptive road segmentation (Iqbal et al., 2023).

Despite significant advances in road segmentation from airborne imagery in previous studies, the task remains an open problem due to several challenges. One significant challenge is the lack of information caused by artifacts such as building shadows, roadside trees, or cars, which can obscure the road surface and hinder accurate segmentation (Lian and Huang, 2022). Another primary issue, known as domain shift, limits the application of already trained models to new study regions due to a significant drop in accuracy (Zhan et al., 2021; Iqbal et al., 2023). Furthermore, many previous studies primarily focused on image segmentation using small, localized images, usually in ideal conditions, from public datasets (Shao et al., 2021). However, when applying segmentation techniques to larger regions, additional challenges such as scalability, heterogeneity, and geometric distortions further complicate the task (W. Chen et al., 2022).

2.2. Road topology

In recent years, several studies have developed various methods to extract road connectivity and networks from aerial and satellite images (Mattyus et al., 2017; Batra et al., 2019). Detecting road curbs is an emerging research topic that has recently gained attention, highlighted by the introduction of the Topo-boundary dataset (Xu et al., 2021b). Initially, road curb detection was formulated as an imitation learning problem (Xu et al., 2021a). Later, a poly-line transformer was proposed for road boundary detection and tested using the Topo-boundary dataset (Hu et al., 2024). Despite the recent successes in curb detection, previous works have primarily relied on supervised learning, which requires large training datasets and faces similar limitations as road segmentation, such as noise occlusion, and scalability issues. These challenges remain to be thoroughly investigated as the topic continues to develop.

While some previous road extraction methods allow for the estimation of road morphology, such as length, curvature, and textures, reliably estimating road width from a bird's-eye view remains challenging due to noise and uncertainties in road extraction (Dai et al., 2019; Grillo et al., 2021). Some previous studies have assumed a fixed width for each road (Ding and Bruzzone, 2020; Manandhar and Marpu, 2018). Although such an assumption can be useful for road network extraction, in reality, road width varies along each road segment. Therefore, methods are required to measure road width accurately. A three-step road width extraction method was proposed by Xia et al. (2017). Another study developed a learning model to estimate road width from remote sensing data and road map centerlines (Luo et al., 2018). Additionally, a previous study applied various data sources, including optical images, geospatial data, and street images, to reduce errors in measuring road width (Grillo et al., 2021). Despite these efforts, accurately measuring road width from an aerial view remains challenging mainly due to various sources of error including inherent remote sensing and geographic errors, overcasts of trees and buildings, and road extraction errors (e.g. segmentation error).

2.3. Uncertainty-aware classification

It is common for road extraction and segmentation algorithms to classify roads erroneously (Lian and Huang, 2022). Uncertainty-aware and probabilistic methods can address these errors and uncertainties in road classification problems. Some previous studies have integrated probabilities into their road detection models using likelihood functions (Iqbal et al., 2023). For example, one study used the Mahalanobis distance as a probability measure to assess the likelihood of a pixel being classified as a road (Miao et al., 2014), while another employed a Gabor filter to define a road probability estimator, identifying a pixel's membership in the road class (Lian and Huang, 2022).

Given the complexities and potential errors in remote sensing data and road detection, adopting uncertainty-aware methods is crucial for improving reliability in challenging scenarios. Several studies have implemented Bayesian modeling in remote sensing data classification (Borges et al., 2011; Li et al., 2011; Golipour et al., 2016). Additionally, recent studies have applied uncertainty-aware methods for road detection in autonomous navigation (Chang et al., 2022; Kim et al., 2024).

Several studies have explored uncertainty-aware approaches for road extraction and measurement from remote sensing data, though they remain relatively few. One study applied Markov random fields (MRF) for road network extraction by fusing multiple data sources (Perciano et al., 2016). Another utilized a Bayesian fusion model to extract roads from synthetic aperture radar (SAR) images (Xu et al., 2017). Additionally, an uncertainty-aware conflation method was proposed for centerline map extraction, applied in railroad data (Lin and Chiang, 2018). With advances in computer vision and deep learning, the use of traditional uncertainty-aware classification models in road segmentation and extraction has declined. However, these methods remain valuable, particularly where uncertainty quantification is critical. A recent study employed a Bayesian neural network for object detection in remote sensing (Sharifuzzaman et al., 2024).

Bayesian classifiers are uncertainty-aware models that apply Bayes' theorem to estimate the probability of a hypothesis, thereby allowing for the estimation of uncertainty in model predictions (Gelman et al., 2013). Bayesian logistic regression (BLR) is one of the well-established methods and has been widely applied across various domains (Dayaratna et al., 2022). BLR is particularly advantageous when data is limited, as it enables the incorporation of prior knowledge to stabilize estimates and improve model performance under conditions of sparse or noisy data (Asanya et al., 2023).

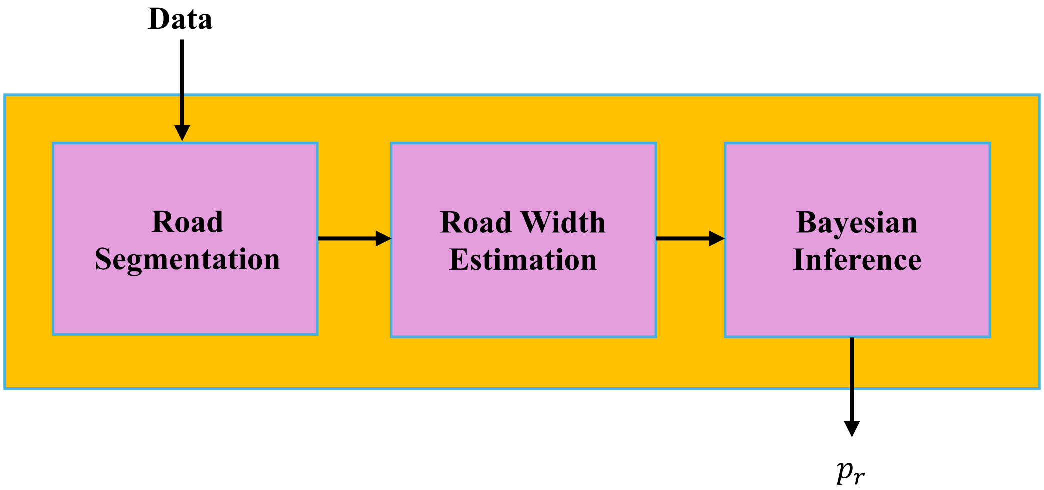

Fig. 1. The workflow of the GUARD.

3. Materials and methods

The primary goal of this study is to detect road segments that fall below required width standards for emergency planning using remote sensing data. Unlike traditional approaches that aim to estimate a single deterministic road width, this study treats width measurements as noisy observations and formulates the problem as probabilistic classification at the segment level. A road segment is considered substandard if its minimum width falls below a required threshold set by emergency management authorities. The inherent noise in remote sensing data complicates this task. Regardless of the road measurement technique used, road width estimations are often noisy due to occlusions and misclassified pixels. Therefore, directly inferring the minimum width along a road segment is not feasible, leading us to formulate the problem as a classification task, with the aim of capturing the latent state of the measurements. Additionally, a Bayesian model is applied to account for uncertainties in the input data and measurements.

The proposed GUARD in this study consists of three main components, as demonstrated in Fig. 1. First, a road segmentation is applied to extract road regions from airborne imagery. Next, the segmented image is used to estimate road width. A Bayesian model is then applied to infer the posterior predictive distribution of road classes.

3.1. Problem formulation

Let the road network be partitioned into R road segments, indexed by $r = 1, \dots, R$. For each segment r, GUARD produces a set of width estimates by sampling cross-sections along the segment using remote sensing-derived road boundaries. Let

$$\hat{\mathbf{w}}_r = \{\hat{w}_{r,1}, \hat{w}_{r,2}, \dots, \hat{w}_{r,n_r}\} \tag{1}$$

denote the collection of n_r sampled width estimates along segment r.

Let $w_{\min}$ denote the minimum required road width (defined by the applicable emergency access standard). A road segment is considered substandard if at least one location along the segment is narrower than $w_{\min}$. We define the (unknown) ground-truth class label $y_r \in \{0, 1\}$ as

$$y_r = \begin{cases} 1, & \text{if } \min(\mathbf{w}_r) < w_{\min}, \\ 0, & \text{otherwise,} \end{cases} \tag{2}$$

where $\mathbf{w}_r$ denotes the true (unobserved) width profile of segment r.

Because only noisy estimates $\hat{\mathbf{w}}_r$ are available from remote sensing, our objective is to estimate, for each segment,

$$p_r \;=\; P\left(y_r = 1 \,\middle|\, \hat{\mathbf{w}}_r\right), \tag{3}$$

which represents the probability that segment r is substandard given the observed width samples. In subsequent sections, we describe how GUARD extracts road regions, constructs $\hat{\mathbf{w}}_r$, and predicts p_r using uncertainty-aware modeling.

3.2. Road segmentation

Road segmentation is used to extract candidate road regions from airborne remote sensing data prior to road width estimation. Numerous approaches have been developed for this task, including deep learning–based methods, semi-supervised and weakly supervised models, and rule-based or clustering-based techniques (Lian et al., 2020), each with different data and annotation requirements. In this study, due to the lack of dense labeled training data in the study area, we employ a multi-modal conditional unsupervised (MCU) segmentation approach that integrates airborne optical imagery, LiDAR-derived elevation data, and sparse user-provided seed points to distinguish road and non-road surfaces. The method combines spectral clustering with simple geometric and elevation constraints derived from road centerlines and a digital surface model to reduce false detections caused by shadows and surrounding land cover. The output of this step is a binary road mask identifying candidate road pixels, which serves as the sole input required by subsequent components of the GUARD framework. Importantly, GUARD is not tied to a specific segmentation algorithm: any road segmentation method that produces sufficiently accurate road masks for the study area of interest can be used without modification to the remaining steps. Implementation details of the MCU segmentation approach used in this study are provided in Appendix.

3.3. Road width estimation

Road width is estimated by uniformly sampling cross-sections along each extracted road segment using the binary road mask obtained from the segmentation step. For each road segment, a centerline representation is used to define sampling locations at regular spatial intervals. At each sampling location, a line perpendicular to the local road direction is constructed and intersected with the segmented road region. The length of the intersection between this perpendicular line and the road mask provides a local estimate of road width. The width estimation procedure was implemented as a GIS-based tool using QGIS and Python, enabling integration with standard geospatial workflows. The procedure yields a set of width estimates for each road segment, reflecting spatial variability along the segment length. Because road segments differ in length and geometry, the number of valid width measurements varies between segments. Measurements are discarded when the perpendicular cross-section does not intersect the road region consistently, which may occur due to segmentation gaps, occlusions, or local misalignment between the road mask and the centerline.

The resulting collection of width estimates for each segment provides a good approximation but is inherently affected by noise arising from segmentation errors, shadows, vegetation, and geometric distortions in the remote sensing data. Rather than attempting to infer a single deterministic width value, these width samples are treated as noisy observations of an underlying width profile. This motivates the use of an uncertainty-aware Bayesian classification framework in the subsequent step, which explicitly accounts for variability and measurement uncertainty when identifying substandard road segments.

3.4. Bayesian logistic regression with moment features

Road width measurements derived from remote sensing are affected by noise and uncertainty arising from segmentation errors, occlusions, and geometric distortions. To account for these uncertainties while classifying road segments as standard or substandard, we adopt a Bayesian logistic regression (BLR) model. While we do not explicitly model measurement noise at the level of individual width observations, uncertainty is incorporated through the variability of sampled width measurements, summarized via moment-based features, and through Bayesian inference, which provides posterior predictive probabilities for classification. Prior to Bayesian inference, a frequentist logistic regression (FLR) model is used as a baseline to guide prior specification and provide a reference for model evaluation.

3.4.1. Moment-based feature transformation

Collecting labeled road width data is costly and limited, whereas remote sensing enables dense sampling of width estimates along each road segment. Directly using all width samples as model inputs would lead to an over-parameterized problem and increase the risk of overfitting. To address this issue, we summarize the set of width estimates for each road segment using a fixed-length vector of statistical moments.

Let $\hat{\mathbf{w}}_r = \{\hat{w}_{r,1}, \hat{w}_{r,2}, \dots, \hat{w}_{r,n_r}\}$ denote the set of width samples for road segment r. The sample mean is computed as $\mu_r = \frac{1}{n_r}\sum_{j=1}^{n_r} \hat{w}_{r,j}$. Higher-order normalized central moments are then calculated as

$$m_{r,k} = \frac{\frac{1}{n_r}\sum_{j=1}^{n_r}(\hat{w}_{r,j} - \mu_r)^k}{\left(\frac{1}{n_r}\sum_{j=1}^{n_r}(\hat{w}_{r,j} - \mu_r)^2\right)^{k/2}}, \qquad k \geq 2. \tag{4}$$

In this study, moments up to order $k = 4$ are used, corresponding to variance, skewness, and kurtosis. These quantities form a fixed-dimensional feature vector $\boldsymbol{\omega}_r = [\mu_r, m_{r,2}, m_{r,3}, m_{r,4}]^\top$, which captures both the typical width and the variability of measurements along the segment. This moment-based representation provides a compact and uncertainty-aware summary of variable-length width samples and enables consistent modeling across road segments.

3.4.2. Frequentist logistic regression baseline

As a baseline model, frequentist logistic regression is applied to relate the moment-based features $\boldsymbol{\omega}_r$ to the binary road class label y_r. The probability that a segment is substandard is modeled as

$$P(y_r = 1 \mid \boldsymbol{\omega}_r, \boldsymbol{\theta}) = \frac{1}{1 + \exp\left(-(\boldsymbol{\theta}^\top \boldsymbol{\omega}_r + \theta_0)\right)}, \tag{5}$$

where $\boldsymbol{\theta}$ and θ_0 are regression coefficients estimated by maximum likelihood. This model provides a point estimate of classification parameters and serves as a reference for subsequent Bayesian inference.

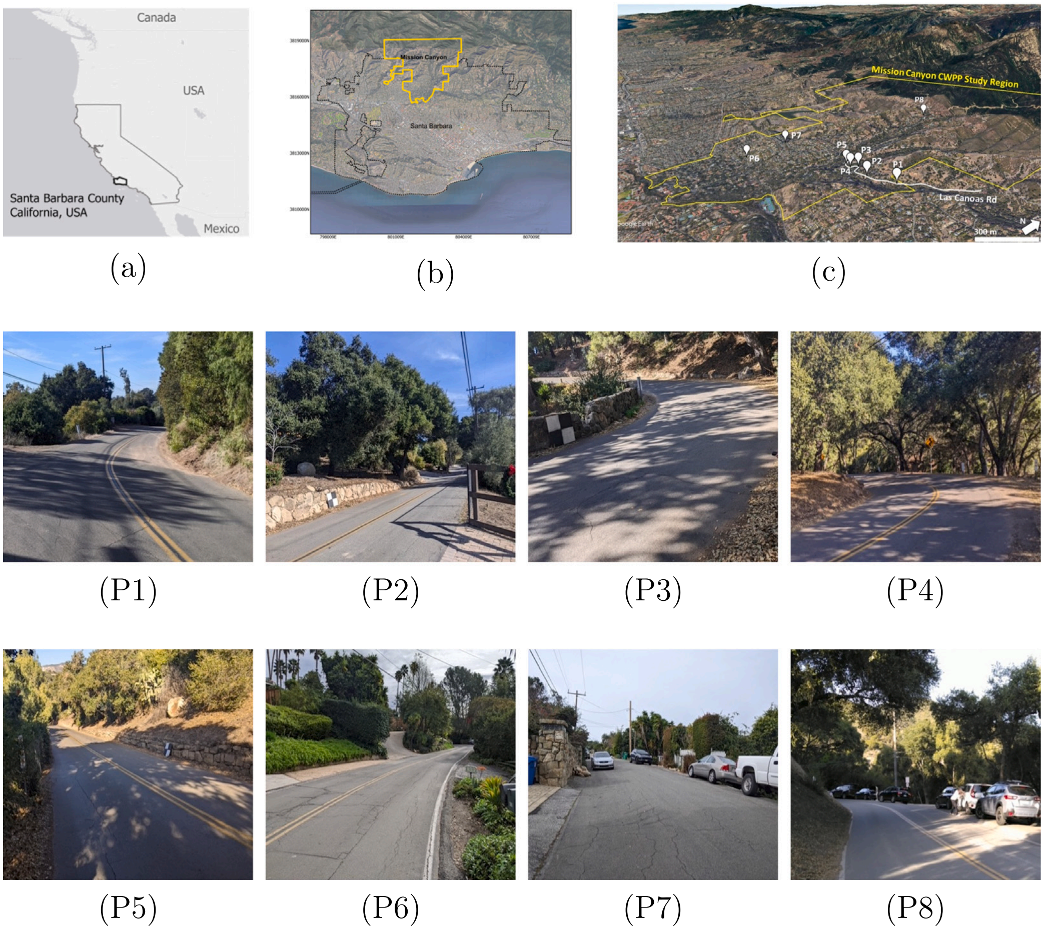

Fig. 2. (a) Location of Santa Barbara County in California, USA, (b) the Mission Canyon study area, (c) a three-dimensional view of the study area showing the location of sample road photos P1-P8.

3.4.3. Bayesian logistic regression

To explicitly quantify uncertainty in both model parameters and predictions, we adopt a Bayesian logistic regression framework. A multivariate normal prior is assigned to the regression coefficients, $\boldsymbol{\theta} \sim \mathcal{N}(\boldsymbol{\mu}, \sigma^2\mathbf{I})$, while the likelihood of the observed class labels is modeled using a Bernoulli distribution with the logistic link function defined above.

Posterior inference is performed using Hamiltonian Monte Carlo (HMC) sampling (Neal, 2012) with the No-U-Turn Sampler (NUTS), which adaptively tunes sampling parameters to improve efficiency (Hoffman, 2014). Samples drawn from the posterior distribution of $\boldsymbol{\theta}$ are used to compute posterior predictive probabilities p_r providing an uncertainty-aware estimate of whether each road segment is substandard. These probabilities form the basis for risk-informed prioritization of road segments for follow-up inspection and emergency planning.

4. Study area and data

4.1. Case study

The developed method was implemented and evaluated using a case study within Santa Barbara County, California, USA. Fig. 2 shows the location, boundary, and a three-dimensional view of the study area along with some road photos. The case study encompasses the Mission Canyon Community Wildfire Protection Plan (CWPP) region, which includes a densely populated region with important cultural and scientific institutions (e.g., the Santa Barbara Botanic Garden) and trailheads to popular back-country recreation areas (e.g., the Tunnel Trailhead to Inspiration Point). Mission Canyon was prioritized for this study due to its recent history of damaging wildfires (i.e., 2009 Jesusita Fire) and continued residential densification, including building of accessory dwelling units (ADUs), which highlights the vulnerability of the region to natural hazards. The study area extends about 3.24 square kilometers (about 800 acres) and the total length of all road segments in the region is about 26.5 km.

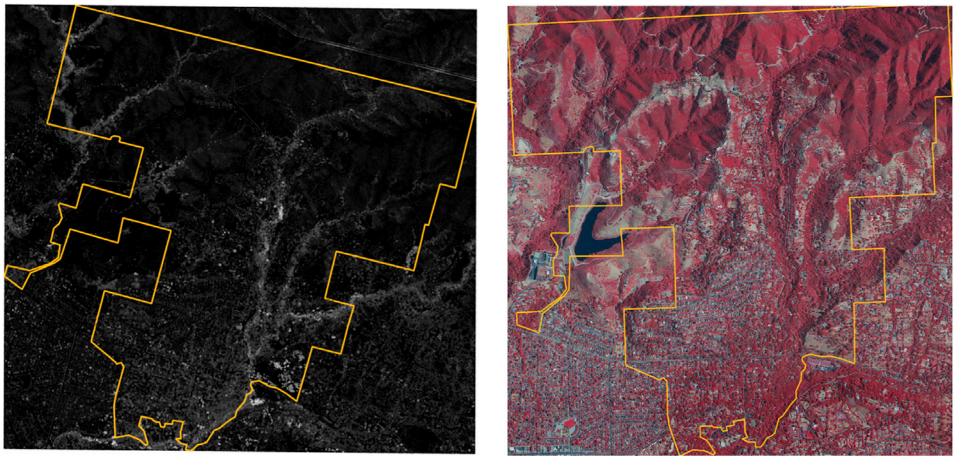

Fig. 3. DSM (left) and NAIP image (right). The DSM image shows terrain height-normalized surface elevations from a 0 m [black] - 40 m [white] range. NAIP image is false color, RGB:NIR-Red-Blue, where NIR highlights vegetation cover.

4.2. Input data

The input data includes a high-resolution airborne optical image, a road centerline map, and LiDAR data. This work uses a National Agriculture Imagery Program (NAIP) image from the United States Department of Agriculture (USDA), covering the study area as of September 2020, which was accessed from the Geospatial Data Gateway (GDG) in July 2022 (United States Department of Agriculture, 2020). The NAIP image was accessed in September 2020, and the near-infrared, red, and green bands were used, with a spatial resolution of 0.6 m. Although RGB images are commonly used for road segmentation, the use of Color-Infrared (CIR) imagery provides better contrast between surfaces, particularly for distinguishing trees and shadows, which enhances the effectiveness of the clustering algorithm. A DSM was created from 2018 LIDAR point cloud data from the United States Geological Survey (USGS) 3D Elevation Program (U.S. Geological Survey, 2018). Raw LiDAR point cloud data were processed into a DSM with 1.0 m spatial resolution. Fig. 3 shows the NAIP image and the DSM. The road center line data was obtained from the Topologically Integrated Geographic Encoding and Referencing (TIGER)/Line produced by the United States Census Bureau (U.S. Census Bureau). All the data are open source and available online. Fig. 4 depicts the TIGER road centerlines in the study area. The centerlines were partitioned into smaller sections with maximum length of 200 m each. Given the focus of this study is on pre-disaster infrastructure assessment, where current road conditions are evaluated to support future emergency planning and preparedness. The use of recent remote sensing imagery and data reflects the current state of the road network, enabling identification of potentially substandard segments under present conditions.

4.3. Ground-truth measurements

To train and test the performance of the model, we conducted in-situ road width measurements for 42 road segments. Road width was measured along target segments using a Bosch GLM165-22 laser distance meter, taking at least three measurements per road segment at intervals of approximately 60–70 meters apart during November and December 2023. The minimum measurement was used to label roads that do not meet the minimum requirement road width. After collecting road segment widths, they were compared with the Santa Barbara County Fire Department (SBCFD)'s road width standards (Division, 2023). For two-way roads without curbside parking, minimum design standard widths were 24 ft (7.3 m) for urban streets (10 ft (3.0 m) wide traffic lanes, with 2 ft (0.61 m) wide shoulders on either side), and 20 ft (6.1 m) for private or rural roads (Division, 2023). For real-world applicability, 20 ft (6.1 m) is widely considered the absolute minimum two-way road width for safe evacuation planning and emergency equipment access. In this study, we used a 6 m threshold, below which roads were classified as substandard width.

4.4. Training, evaluation, and testing datasets

Collecting in-situ road width data is challenging. The data collection process is costly and time-consuming, with concerns and limitations related to privacy, traffic flow, worker safety, accessibility, and required operational permissions. On the other hand, training a classifier requires an extensive amount of data. To prepare the initial datasets for training and testing the models, we used the remote sensing measurements for each road segment as inputs and the label from the ground-truth as the observed classes. Every road segment in the initial dataset has about 215 measurement samples along its route on average. We split the initial dataset of 42 road segments into two sets of training and testing with sizes of 22 and 20 road segments, respectively, as shown in Fig. 5 (left). These initial datasets were not directly applied for training the models. Instead, we generated 10,000 synthetic training data derived from the initial training dataset.

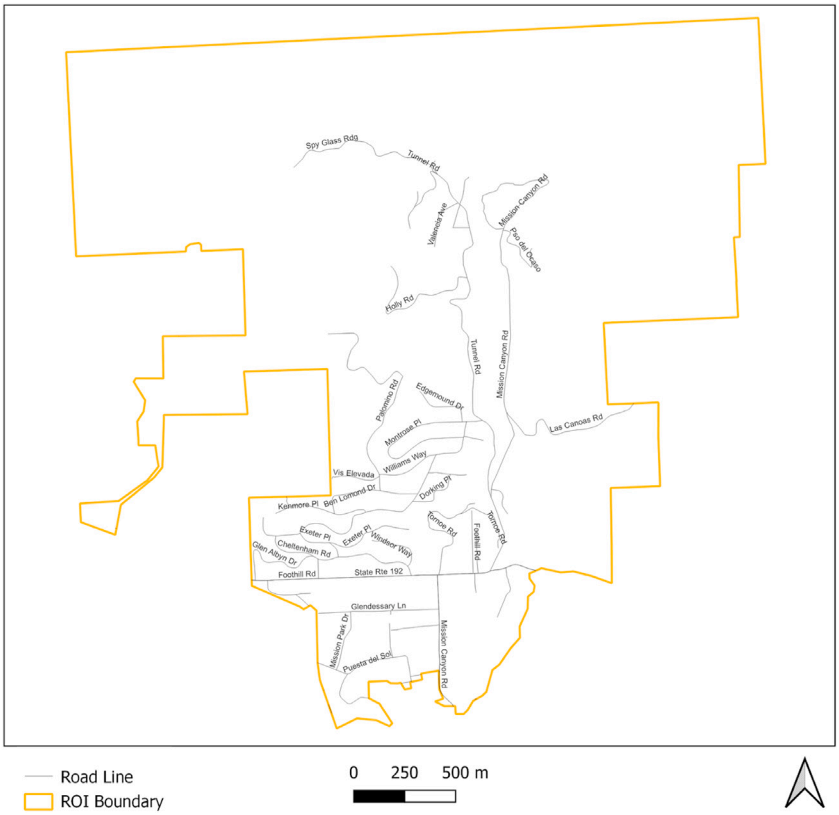

Fig. 4. TIGER centerlines in the study area.

To generate each synthetic road segment, we drew 50 random samples with replacement from a randomly selected road segment in the initial training dataset using a uniform distribution. The feature space of 50% of the synthetic segments was perturbed by adding or subtracting 4% extra samples of length equal to one standard deviation of the segment. Preliminary sensitivity checks indicated that moderate variations in the sampling size and perturbation parameters did not materially affect model performance. The models were trained using only the synthetic data and the initial training dataset were used for evaluation. To ensure the synthetic data represented the actual data, we applied the Kolmogorov–Smirnov (KS) test, with the null hypothesis that the synthetic segments and initial segments come from different distributions. The null hypothesis was not rejected, suggesting that no significant distributional differences were detected between the synthetic and original data under the KS test. Since the synthetic segments are generated by resampling from observed width measurements, the test is used as a diagnostic check to ensure that the resampling and perturbation steps do not introduce unintended distributional distortions. Finally, we used the initial testing dataset directly to test the model.

5. Results

This section presents the empirical results of the proposed GUARD framework. We first examine road width variability along individual road segments and across the road network to illustrate spatial fluctuations in width measurements. We then discuss key challenges associated with road width estimation from remote sensing data, motivating the formulation of the problem as a classification task. Model performance is subsequently evaluated using cross-validation and comparative analyses. Finally, the trained model is applied to estimate the probability of substandard road segments throughout the study area, and the resulting patterns are analyzed in the context of emergency access and evacuation planning for the Mission Canyon community.

5.1. Road width fluctuations

Table 1 lists the total paved road widths (Width) and road widths excluding paved shoulders (carriageway) for sample points P1 to P8, as shown in Fig. 2. The table highlights road width fluctuations both along a single road and among different roads. In Table 1, it is evident that both the carriageway and road width vary significantly along Las Canoas Road (Rd), despite it being a two-lane road throughout its route, as seen in Fig. 2. According to Table 1, the narrowest segment of Las Canoas Rd has a width of 5.5 m, while the widest segment reaches 9.3 m. Additionally, comparing the road widths of Las Canoas, Cheltenham, Vis Elevada,

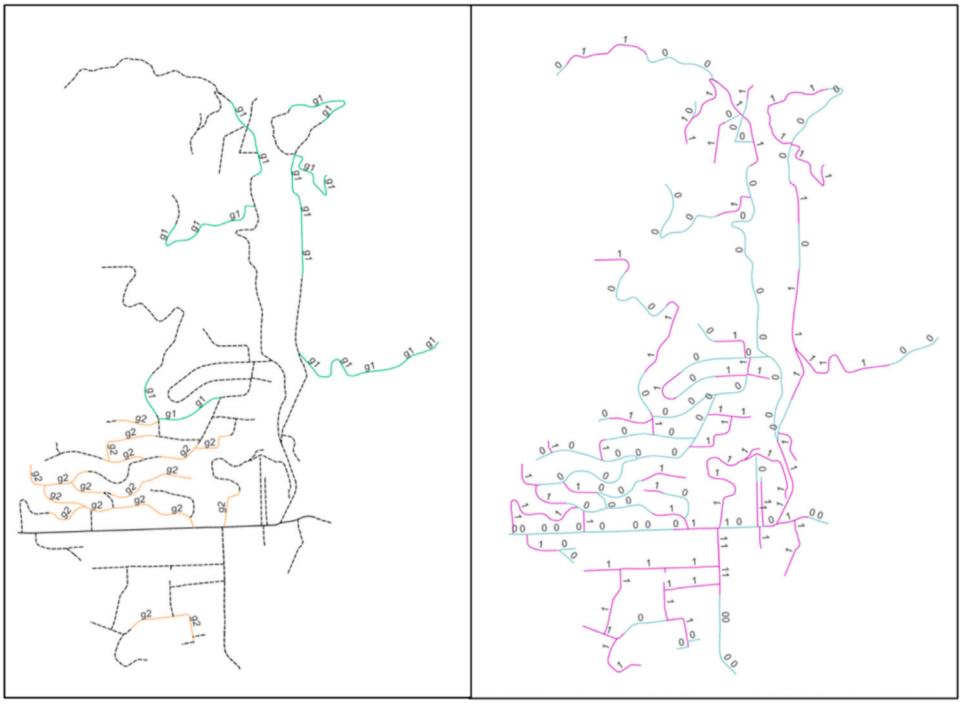

Fig. 5. The initial training and testing road segments prepared based on ground-truth measurements (left) where g1 and g2 refer to the initial training and testing datasets, respectively; and the binary predictions of the BLR (right) where 0 and 1 refer to standard and substandard roads, respectively.

Table 1
Road width and carriageway at points P1-P8.

Point	Street	Carriageway (m)	Width (m)
P1	Las Canoas Rd	6.7	9.3
P2	Las Canoas Rd	5.9	5.9
P3	Las Canoas Rd	4.8	5.5
P4	Las Canoas Rd	6.2	6.8
P5	Las Canoas Rd	5.3	5.7
P6	Cheltenham Rd	6.8	7.9
P7	Vis Elevada	5.3	5.3
P8	Tunnel Rd	5.9*	5.9

Note: The value marked with * does not include the shoulder parking area of 2.8 meter seen in Fig. 2 P8.

and Tunnel Roads reveals significant variations, with widths ranging from 5.3 to 9.3 m, despite all of these roads being two-lane roads. These results highlights the necessity of monitoring road width to detect substandard road segments. In the following results, 'road width' refers to the total paved road width.

5.2. Why classification?

If the measurement error is negligible, we may be able to detect substandard road segments by simply comparing the minimum measurement across the road in a straightforward and deterministic manner. However, this simple method is hardly effective when measuring road width using remote sensing due to various sources of uncertainty. Fig. 6 demonstrates an example of noise caused by vegetation covering significant portions of roads.

Fig. 7 depicts the segmented image. In the case study, for each road segment, we extracted its minimum measurement, referred to as the narrowest cross along a road segment from the segmented image. The minimum, average, and standard deviation of these narrowest crosses are 0.04, 2.42, and 2.31 m, respectively, for all road segments in the study area. Clearly, these measurements do not reflect the actual road widths, as it is unlikely that any road has a width of 0.04 m along its route in the study area.

Fig. 8 visualizes the sample measurements from the developed method along a road segment. It is seen that the road width measurement method in this study has successfully sampled the visible sections of a road segment. However, noise from vegetation is evident. Additionally, slight noise due to road margins, concrete sides, and driveways contributes to the overall measurement noise.

Fig. 6. Occlusion due to dense vegetation (red regions) and shadows that obscures the road from a bird's-eye viewpoint (green lines depict centerlines).

Fig. 7. Segmented image extracted from the MCU algorithm.

As a result, determining whether a road segment's width is below a certain threshold using these noisy remote sensing measurements is challenging. Therefore, we applied a Bayesian classification to detect substandard roads.

5.3. Performance analysis

Given the high level of noise and uncertainty in the remote sensing measurements of road width, we aimed to conduct a probabilistic prediction. Therefore, the primary approach was to use Bayesian logistic regression (BLR). To evaluate the performance of the applied BLR and set its hyperparameters, we used frequentist logistic regression (FLR) as the base model. Table 2 lists the

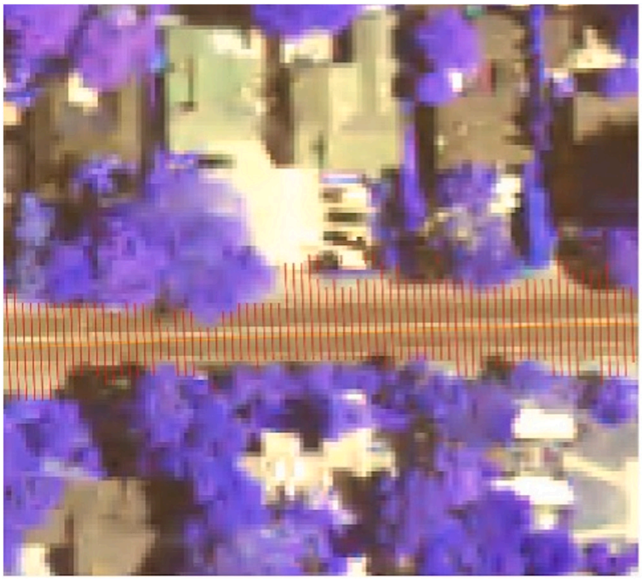

Fig. 8. An example of applied road width measurements (red lines) on part of a road segment.

Table 2
Evaluation (eval) and testing (test) metrics of BLR and FLR.

Model	Accuracy	Precision	Recall	F1 Score
BLR (Eval)	86.4	91.0	83.3	87.0
FLR (Eval)	86.4	91.0	83.3	87.0
BLR (Test)	80.0	75.0	90.0	81.8
FLR (Test)	80.0	75.0	90.0	81.8

evaluation (eval) and testing (test) metrics of the BLR and FLR. For the BLR, we used a normal distribution with $\mu = 0$ and $\sigma = 0.5$ as the prior for θ. These priors were set by evaluating the performance of the BLR against that of the FLR.

Furthermore, both models have achieved good predictive power in classifying the datasets despite the limited amount of available data. The models are consistent between the evaluation and testing datasets. The small differences are primarily due to the dataset size, where a single prediction carries significant weight regarding the percentages. The success of the models in correctly classifying the road segments is more evident when considering the confusion matrices, as shown in Fig. 9, where it is seen that the BLR has predicted most of the road segments correctly. This study was motivated by the needs of local emergency planning agencies seeking a cost-effective preliminary assessment tool to identify potentially substandard road segments for targeted follow-up inspection. Given the nature of our problem, recall is the most important metric, and the models have achieved a recall of 83% and 90% for the evaluation and testing datasets, respectively.

5.4. Cross validation

Cross-validation was applied to ensure that the model's performance was consistent for unseen data and to evaluate its generalizability. For cross-validation, we followed the same procedure to train the model using synthetic data, but instead of using the initial training segments, we generated synthetic data by drawing samples from the testing segments. Table 3 lists the metrics for both BLR and FLR.

Comparing Tables 2 and 3, it is observed that the model performed well with consistent prediction power. There was a slight drop 85% to 80% for accuracy, but given the limited number of dataset observations, that caused the percentage ratio associated with only one mistake to be high, the results were robust. We did not observe a severe drop in accuracy or the performance of the models.

5.5. Inference

The trained BLR was applied to classify the entire study area. There were a total of 171 road segments in the study area, out of which 22 were used for training and 20 for testing, as explained above.

Fig. 5 (right) demonstrates the binary classes for each road segment. According to the binary classification, 83 road segments (52% of the total) in the study area experienced a narrow passage along their route. Fig. 10 shows the likelihood that a road segment

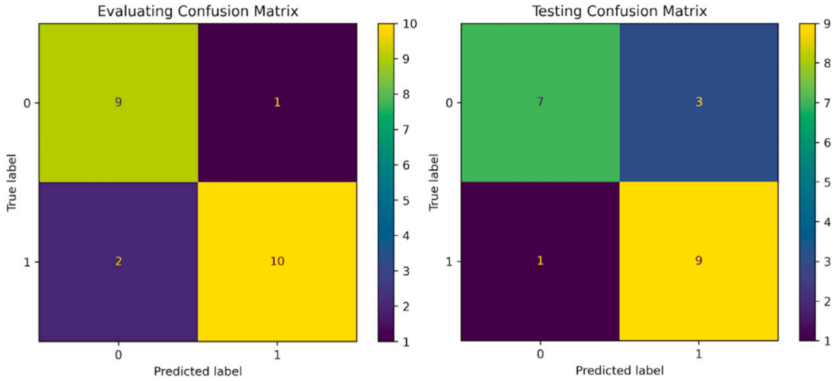

Fig. 9. Confusion matrices of evaluation and testing datasets for the BLR (labels 0 and 1 refer to standard and substandard road segments, respectively).

Table 3
Evaluation (eval) and testing (test) metrics of BLR and FLR for cross validation.

Model	Accuracy	Precision	Recall	F1 Score
BLR (Eval)	85.0	81.2	90.0	85.7
FLR (Eval)	85.0	81.2	90.0	85.7
BLR (Test)	72.3	81.2	75.0	78.2
FLR (Test)	72.3	81.2	75.0	78.3

belongs to the substandard class (class 1). With 90% and 95% confidence intervals, 23 and 12 road segments were detected to have a narrow route, respectively. The inference predictions aligned well with our in-situ inspections of the study area, demonstrating the successful performance of the developed model, although occasional misclassifications were observed.

6. Discussion

6.1. Mission canyon consideration

According to Fig. 5 (right), which presents the binary classification results, it is concerning that 52% of the road segments in the study area are detected to have passages narrower than 6 m. While a small portion of the roads classified as substandard might be misclassified, the overall ratio would likely remain high even after accounting for potential classification errors. Moreover, this ratio aligns with the ground-truth data, where more than half of the road segments indeed experience narrow passages.

Several major roads in the area experience narrow segments along their routes. These narrow sections can easily congest traffic, spreading congestion throughout the region during an emergency evacuation and limiting emergency vehicle access. In addition to the model results, our in-situ measurements and inspections of the area confirm many narrow passages (6 m or less) along study area roads. It is worth mentioning that the prediction is error-prone, and the classification of a road segment as substandard has to be considered in the context of the road's location and use within its broader network. However, the proposed method and results can serve as a preliminary study to identify road segments that require more careful, in-situ inspection in follow-up operations, thereby reducing the cost of monitoring and planning.

During Red Flag conditions, fewer vehicles are permitted in the area, reflecting awareness of the evacuation challenges posed by narrow roads. Measures such as restricted parking and the closure of larger institutions aim to reduce evacuation risks. These efforts also underscore the need for conducting such analyses, facilitating targeted mitigation strategies and improved evacuation planning.

6.2. GUARD consideration

One of the key advantages of the proposed GUARD method in this study is its adaptability to other segmentation and measurement techniques. The classifier developed does not rely on any specific assumptions about the road width samples. Moreover, remote sensing measurements are inherently prone to errors at multiple levels. For example, enhancing the accuracy of road width estimation from a segmented image does not necessarily result in higher overall accuracy due to segmentation errors. Similarly, improving segmentation accuracy does not guarantee better results due to inherent sensing errors. Therefore, the proposed uncertainty-aware model offers a robust approach to address these uncertainties.

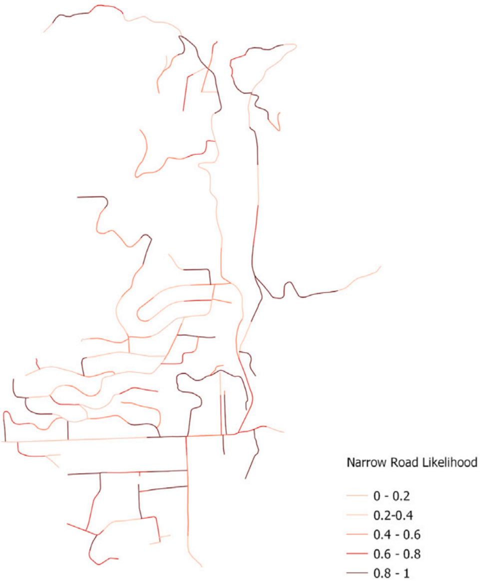

Fig. 10. Likelihood of substandard road segments (total 171 road segments).

The results demonstrate that the model can be effectively trained with a limited dataset, making it easier to apply in new regions, as only a small amount of data is required for calibration. In this study, we used distinct regions for training and testing datasets, as shown in Fig. 5. However, further investigation is necessary to confirm the model's generalizability. To enhance its applicability, future studies should focus on collecting additional data across diverse landscapes and updating the model to improve its generalizability. Nonetheless, for very wide and very narrow roads, the model is expected to perform well on new (unseen) datasets, provided that segmentation and road width measurements have minimal errors. Generalizability may be more challenging for road segments with limited visibility or those with widths very close to emergency management, access or design code thresholds in new landscapes.

6.3. Future work

This study focuses on formulating substandard road detection as a classification problem using noisy remote sensing–derived width measurements. The primary objective is to provide a preliminary screening tool to identify potentially substandard road segments for follow-up inspection. Although current work demonstrates the feasibility of this approach, it does not explicitly address decision-theoretic aspects such as cost-sensitive prioritization of inspections. These aspects are highly dependent on local emergency management policies, available resources, and operational risk tolerance and therefore remain important directions for future research.

7. Conclusion

In this study, a novel geospatial uncertainty-aware road width detection (GUARD) method was developed to classify and detect substandard roads for natural hazards mitigation and management using remote sensing data. The proposed GUARD consists of three steps. First, a road segmentation was conducted. Next, the segmented image was used to estimate road width. A Bayesian model was presented to infer the posterior predictive distribution of substandard roads. Additionally, to evaluate the developed model and assess road width conditions, ground-truth data were collected in Mission Canyon, Santa Barbara, USA.

Both the ground-truth observations and the classification model revealed that more than half of the road segments in the study area had passages narrower than emergency management access standards. This finding raises concerns about many similar older wildland-urban interface neighborhoods across the United States. While infrastructure development and road expansion may not always be feasible, monitoring and detecting weak spots are crucial for wildfire and flood hazard management and evacuation planning. The proposed method can help reduce monitoring costs by initially identifying areas where further investigation and more careful inspection are necessary.

CRediT authorship contribution statement

Ryan Solgi: Writing – review & editing, Writing – original draft, Software, Methodology, Investigation, Formal analysis, Conceptualization. **Marc Mayes:** Writing – review & editing, Writing – original draft, Software, Methodology, Investigation, Formal analysis, Conceptualization. **Rob Hazard:** Writing – review & editing, Investigation, Conceptualization. **Hugo A. Loáiciga:** Writing – review & editing, Conceptualization.

Ethical statement

In accordance with Elsevier's policies on publishing ethics (https://www.elsevier.com/about/policies-and-standards/publishing-ethics#4-duties-of-authors), this study did not involve human participants, human data, personal identifying information, animal subjects, clinical research, or interventions. All remote sensing datasets used are publicly available, open-access geospatial products. Field measurements were limited to non-invasive observations of public road infrastructure and did not involve interactions with identifiable individuals. Therefore, ethical approval and informed consent were not applicable to this research.

Funding

This work was supported in part by a National Fish and Wildlife Foundation (NFWF), United States National Coastal Resilience Grant (0318.19.070225). This work was also partially supported by the Earth Research Institute (ERI) and the Department of Geography at the University of California-Santa Barbara (UCSB), Santa Barbara, CA, USA.

Declaration of competing interest

The authors declare the following financial interests/personal relationships which may be considered as potential competing interests: Marc Mayes reports financial support was provided by National Fish and Wildlife Foundation (NFWF). If there are other authors, they declare that they have no known competing financial interests or personal relationships that could have appeared to influence the work reported in this paper.

Acknowledgments

We would like to thank Max Moritz for his guidance on framing the research challenge addressed in this paper. The research collaboration among authors Solgi, Mayes and Hazard is an affiliated activity of the Regional Wildfire Mitigation Program (RWMP) in Santa Barbara, California.

Appendix

Road segmentation is used to extract candidate road regions from airborne remote sensing data prior to road width estimation. While deep learning approaches have shown strong performance for road extraction, they typically require large labeled datasets, which are not available in the study area. To address this limitation, we adopt a multi-modal conditional unsupervised (MCU) segmentation strategy that combines clustering with simple geometric and elevation constraints.

The MCU method integrates three sources of information: (i) an airborne optical image, (ii) a digital surface model (DSM) derived from LiDAR data, and (iii) a sparse set of user-provided seed points indicating representative road and shadow locations. The goal is to classify image pixels into road and non-road classes without relying on dense manual annotations.

Clustering is first applied to the optical image to group pixels with similar spectral characteristics. Let $\mathbf{X} \in \mathbb{R}^{n_x \times n_y \times n_b}$ denote the optical image with n_b spectral bands. Applying K-means clustering partitions the image into K spectral clusters. Clusters that contain road-labeled seed points are identified as candidate road clusters, while clusters containing shadow-labeled seed points are identified separately to account for illumination effects.

To reduce false positives caused by shadows and non-road surfaces, spatial and elevation constraints are imposed using road centerlines and LiDAR-derived elevation data. Let $\mathcal{M}$ denote the set of road centerline points and let $T(\cdot)$ be a geometric transformation that maps image pixels to the coordinate system of $\mathcal{M}$. For each pixel (i, j), the minimum distance to the road centerline is computed as

$$d_{ij} = \min_{\mathbf{q}\in\mathcal{M}} \|T(i, j) - \mathbf{q}\|. \tag{A.1}$$

Pixels belonging to candidate road clusters are classified as road pixels if their distance to the centerline is below a predefined threshold ξ_d. For pixels belonging to shadow-related clusters, an additional elevation consistency check is applied. Let $E(\cdot)$ denote elevation values from the DSM. A shadow pixel is reclassified as road if the elevation difference between the pixel and its nearest centerline point satisfies

$$|E(T(i, j)) - E(\mathbf{q}^*)| \leq \xi_e, \tag{A.2}$$

where $\mathbf{q}^*$ is the closest centerline point to (i, j).

The final output of the segmentation step is a binary road mask $\mathbf{B} \in \{0, 1\}^{n_x \times n_y}$ where 1 indicates road pixels and 0 denotes non-road pixels. A schematic overview of the MCU segmentation workflow is shown in Fig. A.11.

The proposed segmentation approach is designed for publicly available airborne optical and LiDAR data in the United States. While alternative segmentation methods could be employed depending on data availability, the subsequent steps of the GUARD framework require only a binary road mask. As a result, the overall methodology is flexible and can accommodate different segmentation techniques without modification to the remaining components.

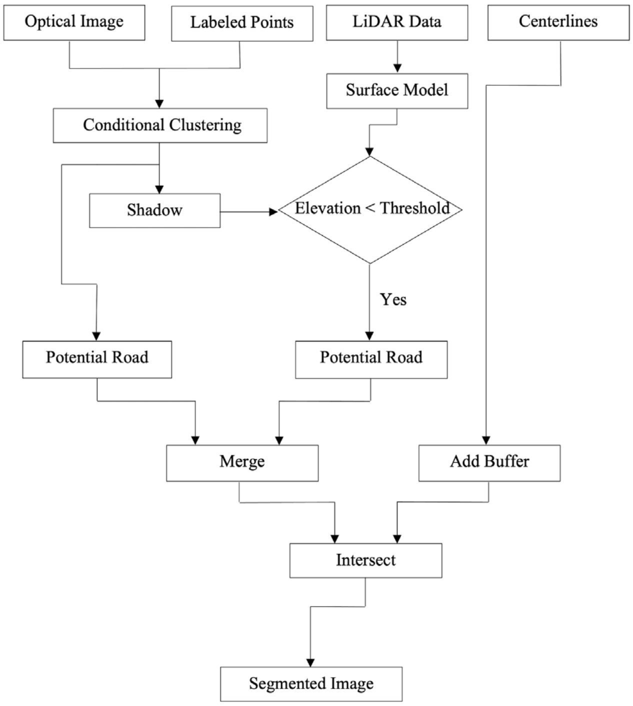

Fig. A.11. A flowchart of the multi-modal conditional unsupervised (MCU) learning for road segmentation.

Data availability

This work uses a National Agriculture Imagery Program (NAIP) image from the United States Department of Agriculture (USDA), covering the study area as of September 2020, which was accessed from the Geospatial Data Gateway (GDG) in July 2022 (United States Department of Agriculture, 2020). A DSM was created from 2018 LIDAR point cloud data from the United States Geological Survey (USGS) 3D Elevation Program (U.S. Geological Survey, 2018). The road center line data was obtained from the Topologically Integrated Geographic Encoding and Referencing (TIGER)/Line produced by the United States Census Bureau (U.S. Census Bureau).

References

Abdollahi, A., Pradhan, B., Shukla, N., Subrata, C., Alamri, A., 2020. Deep learning approaches applied to remote sensing datasets for road extraction: A state-of-the-art review. Remote. Sens. 12, 1444.
Aldahlawi, R.Y., Akbari, V., Lawson, G., 2024. A systematic review of methodologies for human behavior modelling and routing optimization in large-scale evacuation planning. Int. J. Disaster Risk Reduct. 110.
Alizadeh, N., Mahdianpari, M., Hemmati, E., Marjani, M., 2024. FusionFireNet: A CNN-LSTM model for short-term wildfire hotspot prediction utilizing spatio-temporal datasets. Remote. Sens. Appl.: Soc. Environ. 37, 101436. http://dx.doi.org/10.1016/j.rsase.2024.101436.
Asanya, K.C., Kharrata, M., Udom, A.U., Torsen, E., 2023. Robust Bayesian approach to logistic regression modeling in small sample size utilizing a weakly informative student's t prior distribution. Comm. Statist. Theory Methods 52 (2).
Batra, A., Singh, S., Pang, G., Basu, S., jawahar, C., Paluri, M., 2019. Improved road connectivity by joint learning of orientation and segmentation. IEEE/CVF Conf. Comput. Vis. Pattern Recognit. (CVP).
Beyki, S.M., Lopes, A.M.G., Santiago, A., 2025. Improving wildfire simulation accuracy using satellite active fire data for interval reinitialization and rate of spread adjustment. Remote. Sens. Appl.: Soc. Environ. 39, 101648. http://dx.doi.org/10.1016/j.rsase.2025.101648.
Bhattacharyya, A., Morshedi, M., Hastak, M., 2023. A clustering-classification approach in categorizing vulnerability of roads and bridges using public assistance big data. Int. J. Disaster Risk Reduct. 84.
Borges, J.S., Bioucas-Dias, J.M., Marcal, A.R.S., 2011. Bayesian hyperspectral image segmentation with discriminative class learning. IEEE Trans. Geosci. Remote Sens. 49 (6).
Chang, Y., Xue, F., Sheng, F., Liang, W., Ming, A., 2022. Fast road segmentation via uncertainty-aware symmetric network.
Chen, Z., Deng, L., Luo, Y., Li, D., Junior, J.M., Goncalves, W.N., Nurunnabi, A.A.M., LI, J., Wang, C., Li, D., 2022. Road extraction in remote sensing data: A survey. Int. J. Appl. Earth Obs. Geoinf. 112, 102833.
Chen, H., Li, Z., Wu, J., Xiong, W., Du, C., 2023. SemiRoadExNet: A semi-supervised network for road extraction from remote sensing imagery via adversarial learning. ISPRS J. Photogramm. Remote Sens. 198.
Chen, H., Peng, S., Du, C., Li, J., Wu, S., 2022. SW-GAN: Road extraction from remote sensing imagery using semi-weakly supervised adversarial learning. Remote. Sens. 14 (17).
Chen, Y., Shafi, S.Y., Chen, Y., 2020. Simulation pipeline for traffic evacuation in urban areas and emergency traffic management policy improvements through case studies. Transp. Res. Interdiscip. Perspect. 7.

Chen, Z., Wang, C., Li, J., Xie, N., Han, Y., Du, J., 2021. Reconstruction bias U-net for road extraction from optical remote sensing images. IEEE J. Sel. Top. Appl. Earth Obs. Remote. Sens. 14.

Chen, W., Zhou, G., Liu, Z., Li, X., Zheng, X., Wang, L., 2022. NIGAN: A framework for mountain road extraction integrating remote sensing road-scene neighborhood probability enhancements and improved conditional generative adversarial network. IEEE Trans. Geosci. Remote Sens. 60.

Dai, J., Zhu, T., Zhang, Y., Ma, R., Li, W., 2019. Lane-level road extraction from high-resolution optical satellite images. Remote. Sens. 11, 2672.

Dayaratna, K., Crosson, J., Hubbard, C., 2022. Closed form bayesian inferences for binary logistic regression with applications to american voter turnout. Stats 5 (4).

Ding, L., Bruzzone, L., 2020. DiResNet: Direction-aware residual network for road extraction in VHR remote sensing images. IEEE Trans. Geosci. Remote. Sens. 59 (12).

Division, F.P., 2021. Development standard-#1: Fire apparatus access. St. Barbar. Cty. Fire Dep.

Division, F.P., 2023. Development standard-#1: Fire apparatus access. St. Barbar. Cty. Fire Dep.

Dye, A.W., Kim, J.B., McEvoy, A., Fang, F., Riley, K.L., 2021. Evaluating rural Pacific northwest towns for wildfire evacuation vulnerability. Nat. Hazards

Effinger, R., 2021. Traffic modeling of potential emergency wildfire evacuation routes. Caltrans Div. Res. Innov. Syst. Inf.

Gelman, A., Carlin, J.B., Stern, H.S., Dunson, D.B., Vehtari, A., Rubin, D.B., 2013. Bayesian data analysis. CRC Press.

Golipour, M., Ghassemian, H., Mirzapour, F.a., 2016. Integrating hierarchical segmentation maps with MRF prior for classification of hyperspectral images in a bayesian framework. IEEE Trans. Geosci. Remote Sens. 54 (2).

Grillo, A., Krylov, V.A., Moser, G., Serpico, S.B., 2021. Road extraction and road width estimation via fusion of aerial optical imagery, geospatial data, and street-level images. IEEE Int. Geosci. Remote. Sens. Symposium (IGARSS) http://dx.doi.org/10.1109/IGARSS47720.2021.955454.

Hoffman, M.D., 2014. The no-u-turn sampler: Adaptively setting path lengths in Hamiltonian Monte Carlo. J. Mach. Learn. Res. 15, 1593–1623.

Hu, A., Chen, S., Wu, L., Xie, Z., Qiu, Q., Xu, Y., 2021. WSGAN: An improved generative adversarial network for remote sensing image road network extraction by weakly supervised processing.. Remote. Sens. 13 (13).

Hu, Y., Wang, Z., Liu, Y., 2024. PolyRoad: Polyline transformer for topological road-boundary detection. IEEE Trans. Geosci. Remote Sens. 62.

Intergovernmental Panel on Climate Change (IPCC), 2021. Sixth Assessment Report Cycle. Cambridge University Press.

Iqbal, J., Masood, A., Sultani, W., Ali, M., 2023. Leveraging topology for domain adaptive road segmentation in satellite and aerial imagery. ISPRS J. Photogramm. Remote Sens. 206.

Jiang, X., Li, Y., Jiang, T., Xie, J., Wu, Y., Cai, Q., Jiang, J., Xu, J., Zhang, H., 2022. RoadFormer: Pyramidal deformable vision transformers for road network extraction with remote sensing images. Int. J. Appl. Earth Obs. Geoinf.

Karimzadeh, S., Ghasemi, M., Matsuoka, M., Yagi, K., Zulfikar, C.A., 2022. A deep learning model for road damage detection after an earthquake based on synthetic aperture radar (SAR) and field datasets. 15.

Kim, O., Seo, J., Ahn, S., Kim, C.H., 2024. UFO: uncertainty-aware lidar-image fusion for off-road semantic terrain map estimation.

Kirthika, A., Mookambiga, A., 2011. Automated road network extraction using artificial neural network. In: International Conference on Recent Trends in Information Technology. ICRTIT.

Li, J., Bioucas-Dias, J.M., Plaza, A., 2011. Hyperspectral image segmentation using a new Bayesian approach with active learning. IEEE Trans. Geosci. Remote Sens. 49 (10).

Lian, R., Huang, L., 2022. Weakly supervised road segmentation in high-resolution remote sensing images using point annotations. IEEE Trans. Geosci. Remote Sens. 60.

Lian, R., Wang, W., Mustafa, N., Huang, L., 2020. Road extraction methods in high-resolution remote sensing images: A comprehensive review. IEEE J. Sel. Top. Appl. Earth Obs. Remote. Sens. 13.

Lin, H., Chiang, Y.-Y., 2018. An uncertainty aware method for geographic data conflation. Proc. the 7th ACM SIGSPATIAL Int. Workshop Anal. Big Geospatial Data 20–27.

Liu, P., Wang, Q., Yang, G., Li, L., Zhang, H., 2022. Survey of road extraction methods in remote sensing images based on deep learning. PFG–Journal Photogramm. Remote. Sens. Geoinf. Sci. 90.

Luo, L., Zang, Y., Wang, X., Wang, C., Li, J., Wu, S., Liu, Y., 2018. Estimating road widths from remote sensing images. Remote. Sens. Lett. 9 (9), 819–828.

Malama, S., Jana, D., Narasimhan, S., Taciroglu, E., 2024. Integrating vision and lidar based hyperlocal metadata for optimal capacity expansion planning in hillside road networks. Adv. Eng. Informatics 62, 102743. http://dx.doi.org/10.1016/j.aei.2024.102743.

Manandhar, P., Marpu, P.R., 2018. Segmentation based traversing- agent approach for road width extraction from satellite images using volunteered geographic information. Appl. Comput. Informatics 17 (1), 131–152.

Maranghides, A., Link, E., Brown, C.U., Walton, W.D., Mell, W., Hawks, S., 2023. A case study of the camp fire - notification, evacuation, traffic, and temporary refuge areas (NETTRA).. Natl. Inst. Stand. Technol. http://dx.doi.org/10.6028/NIST.TN.2252.

Matkan, A.A., Hajeb, M., Sadeghian, S., 2014. Road extraction from lidar data using support vector machine classification. Photogramm. Eng. Remote Sens. 80 (5).

Mattyus, G., Luo, W., Urtasun, R., 2017. DeepRoadMapper: Extracting road topology from aerial images. Int. Conf. Comput. Vis.

Miao, Z., Wang, B., Shi, W., Zhang, H., 2014. A semi-automatic method for road centerline extraction from vhr images. IEEE Geosci. Remote. Sens. Lett. 11 (11).

Moratalla, J.M., Uma, S.R., 2023. Probabilistic assessment of road accessibility under cascading hazards. Int. J. Disaster Risk Reduct. 91.

Neal, R.M., 2012. MCMC using hamiltonian dynamics.

Niu, C., Nair, D.J., Zhang, T., Dixit, V., Murray-Tuit, P., 2022. Are wildfire fatalities related to road network characteristics? A preliminary analysis of global wildfire cases. Int. J. Disaster Risk Reduct. 80.

Ouyang, M., Zeng, B., Huang, G., 2025. A deep learning method for identifying waterlogging depth on urban roadways from surveillance camera images. Remote. Sens. Appl.: Soc. Environ. 41, 101827. http://dx.doi.org/10.1016/j.rsase.2025.101827.

Perciano, T., Tupina, F., Hirata, R., Cesar, R.M., 2016. A two-level Markov random field for road network extraction and its application with optical, SAR, and multitemporal data. Int. J. Remote Sens. 37 (16).

Rahman, M., Chen, N., Islam, M.M., Dewan, A., Pourghasemi, H.R., Washakh, R.M.A., Nepal, N., Tian, S., Faiz, H., Alam, M., Ahmed, N., 2021. Location-allocation modeling for emergency evacuation planning with gis and remote sensing: A case study of northeast Bangladesh. Geosci. Front..

Sadiq, R., Akhtar, Z., Imran, M., Ofli, F., 2022. Integrating remote sensing and social sensing for flood mapping. Remote. Sens. Appl.: Soc. Environ. 25, 100697. http://dx.doi.org/10.1016/j.rsase.2022.100697.

Salandra, M.L., Nicotri, S., Donvito, G., Italiano, A., Colacicco, R., Miniello, G., Lapietra, I., Roseto, R., Dellino, P., Capolongo, D., 2024. A paradigm shift in processing large UAV image datasets for emergency management of natural hazards. Int. J. Appl. Earth Obs. Geoinf. 132.

Schnebele, E., Tanyu, B.F., Cervone, G., Waters, N., 2015. Review of remote sensing methodologies for pavement management and assessment. Eur. Transp. Res. Rev. 7 (7), http://dx.doi.org/10.1007/s12544-015-0156-6.

Sdraka, M., Dimakos, A., Malounis, A., Ntasiou, Z., Karantzalos, K., Michail, D., Papoutsis, I., 2024. FLOGA: A machine-learning-ready dataset, a benchmark, and a novel deep learning model for burnt area mapping with sentinel-2. IEEE Sel. Top. Appl. Earth Obs. Remote. Sens. 17.

Shamsolmoali, P., Zareapoor, M., Zhou, H., Wang, R., Yang, J., 2021. Road segmentation for remote sensing images using adversarial spatial pyramid networks. IEEE Trans. Geosci. Remote. Sens. 59 (6).

Shao, Z., Zhou, Z., Huang, X., Zhang, Y., 2021. Mrenet: Simultaneous extraction of road surface and road centerline in complex urban scenes from very high-resolution images. Remote. Sens. 13 (239).
Sharifuzzaman, S.A.S.M., Tanveer, J., Chen, Y., Chan, J.H., Kim, H.S., Kallu, K.D., Ahmed, S., 2024. Bayes R-CNN: An uncertainty-awarebayesian approach to object detection in remote sensing imagery for enhanced scene interpretation. Remote. Sens. 16.
Sibandze, P., Kalumba, A.M., Afuye, G.A., Kganyago, M., 2025. Integrating remote sensing data and fully connected convolutional neural networks for flood probability and risk assessment. Remote. Sens. Appl.: Soc. Environ. 39, 101630. http://dx.doi.org/10.1016/j.rsase.2025.101630.
Sommer, L., 2024. Lahaina,äôs deadly wildfire could be a chance to rebuild safer. But will it? https://www.wcbe.org/npr-news/2024-08-08/lahainas-deadly-wildfire-could-be-a-chance-to-rebuild-safer-but-will-it. (last accessed 8 August 2024),
Song, M., Civco, D., 2004. Road extraction using SVM and image segmentation. Photogramm. Eng. Remote Sens. 70 (12).
Song, J., Li, J., Chen, H., Wu, J., 2021. MapGen-GAN: A fast translator for remote sensing image to map via unsupervised adversarial learning. IEEE J. Sel. Top. Appl. Earth Obs. Remote. Sens. 14.
Szpakowskia, D.M., Jensen, J.L.R., Butler, D.R., Chow, T.E., 2021. A study of the relationship between fire hazard and burn severity in grand teton national park, USA. Int. J. Appl. Earth Obs. Geoinf. 98.
Tao, Y., Xu, M., Zhang, F., Du, B., Zhang, L., 2017. Unsupervised-restricted deconvolutional neural network for very high resolution remote-sensing image classification. IEEE Trans. Geosci. Remote Sens. 55 (12).
United States Department of Agriculture, 2020. National agriculture imagery program (NAIP) data. (Geospatial Data Gateway), URL https://datagateway.nrcs.usda.gov/GDGHome_DirectDownLoad.aspx.
U.S. Census Bureau, TIGER/Line Geodatabases. URL https://www.census.gov/geographies/mapping-files/time-series/geo/tiger-geodatabase-file.html.
U.S. Geological Survey, 2018. 3D elevation program (3DEP). (U.S. Department of the Interior), URL https://www.usgs.gov/3d-elevation-program.
Vishwanath, T., et al., 2023. Social media data extraction for disaster management aid. Remote. Sens. Appl.: Soc. Environ. 30, 100961. http://dx.doi.org/10.1016/j.rsase.2023.100961.
Wang, Y., Seo, J., Jeon, T., 2019. NL-LinkNet: Toward lighter but more accurate road extraction with non-local operations. IEEE Geosci. Remote. Sens. Lett.
Wang, W., Yang, N., Zhang, Y., Wang, F., Cao, T., Eklund, P., 2016. A review of road extraction from remote sensing images. J. Traffic Transp. Eng. 3 (3).
Wei, Y., Ji, S., 2022. Scribble-based weakly supervised deep learning for road surface extraction from remote sensing images. IEEE Trans. Geosci. Remote Sens. 60.
Wei, M., Xu, J., 2024. Assessing road network resilience in disaster areas from a complex network perspective: A real-life case study from China. Int. J. Disaster Risk Reduct. 100.
Wolshon, B., 2006. Evacuation planning and engineering for hurricane katrina.
Wolshon, B., Wilmot, C.G., Levitan, M.L., 2005. Review of policies and practices for hurricane evacuation. I: Transportation planning, preparedness, and response. Nat. Hazards Rev. 6.
Wu, S., Chun Du, H.C., Yingxiao Xu, N.G., Jing, N., 2019. Road extraction from very high resolution images using weakly labeled openstreetmap centerline. ISPRS Int. J. Geo-Information (11).
Xia, Z., Zang, Y., Wang, C., Li, J., 2017. Road width measurement from remote sensing images. IEEE Int. Symp. Geosci. Remote. Sensing (IGARSS).
Xu, R., He, C., Liu, X., Chen, D., Qin, Q., 2017. Bayesian fusion of multi-scale detectors for road extraction from sar images. Int. J. Geo-Information 6 (26).
Xu, Z., Sun, Y., Liu, M., 2021a. iCurb: Imitation learning-based detection of road curbs using aerial images for autonomous driving. IEEE Robot. Autom. Lett. 6 (2).
Xu, Z., Sun, Y., Liu, M., 2021b. Topo-boundary: A benchmark dataset on topological road-boundary detection using aerial images for autonomous driving. IEEE Robot. Autom. Lett.
Yin, D., Du, S., Wang, S., Guo, Z., 2015. A direction-guided ant colony optimization method for extraction of urban road information from very-high-resolution images. IEEE Jouranl Sel. Top. Appl. Earth Obervations Remote. Sens. 8 (10).
Zhan, L., Lan, M., Zhang, J., Tao, D., 2021. Stagewise unsupervised domain adaptation with adversarial self-training for road segmentation of remote sensing images. IEEE Trans. Geosci. Remote Sens.
Zhang, Z., Liu, Q., Wang, Y., 2018. Road extraction by deep residual U-net. IEEE Geosci. Remote. Sens. Lett.
Zheng, X., Wang, F., Qi, M., Meng, Q., 2021. Planning remote sensing emergency services: Bridging the gap between remote sensing science and emergency practice in China. Saf. Sci.
Zhong, Z., Li, J., Cui, W., Jiang, H., 2016. Fully convolutional networks for building and road extraction: Preliminary results. In: IEEE International Symposium on Geoscience and Remote Sensing. IGARSS.
Zhou, M., Sui, H., Chen, S., Wang, J., Chen, X., 2020. BT-RoadNet: A boundary and topologically-aware neural network for road extraction from high-resolution remote sensing imagery. ISPRS J. Photogramm. Remote. Sens. 168.